Diurnal active photolocation enhances predator detection in a marine fish

Matteo Santon[1], Pierre-Paul Bitton[1], Jasha Dehm[1,2], Roland Fritsch[1],
Ulrike K. Harant[1], Nils Anthes[1], Nico K. Michiels[1]*

[1]Animal Evolutionary Ecology, Institute of Evolution and Ecology, Department of Biology, Faculty of Science, University of Tübingen, Auf der Morgenstelle 28, 72076 Tübingen, Germany

[2]Current address: School of Marine Studies, Faculty of Science, Technology & Environment, University of the South Pacific, Laucala Bay Rd., Suva, Fiji

*corresponding author

FIGURES included in the text

Nocturnal and deep-sea fish which possess a chemiluminescent subocular search light to detect prey are currently the only known vertebrates to use light for active sensing[1,2]. However, recent findings suggest diurnal fish may also benefit from a form of active photolocation[3]. The triplefin *Tripterygion delaisi,* a small benthic fish[4,5], redirects downwelling sunlight from its irides in a controlled, context-specific manner[3]. This close arrangement between light source and pupil is analogous to that found in bioluminescent fishes[2,6-10] and suggests a specialisation in the induction and detection of retroreflective eyeshine in other organisms[1,3,11]. However, diurnal active photolocation has never been empirically demonstrated. Here we show that experimentally reducing triplefin iris radiance affects how closely they approach a cryptobenthic sit-and-wait predator, a scorpionfish with retroreflective eyes[12]. Triplefins treated with a shading hat, which only prevented iris radiance, approached the predator significantly closer than two controls in replicate laboratory and field experiments. Visual modelling confirmed diurnal active photolocation of scorpionfish is indeed a plausible mechanism under natural light conditions. We conclude that redirection of ambient light can allow a small benthic fish to induce and detect eyeshine in its predator. Given the ubiquity of small fish with light re-directing irides[3,13] and cryptobenthic predators with retroreflective eyes, this newly described form of active sensing is likely to be widespread and offers an additional explanation for the evolution of eye-related reflecting structures.

A prominent anatomical feature of the eye of most fish species is the spherical lens protruding from the pupil. Depending on the exact geometry, light striking the top of the lens can be focused as a bright spot on the iris. Consequently, downwelling light is redirected sideways in the plane of vision. Previous work showed that the production of this so-called ocular spark is a behaviourally-controlled mechanism (Fig. 1a-c)[3] and hypothesized that it produces sufficient light to improve visual detection of strong reflectors in potential predators. For example, retroreflective eyes, which are focusing eyes with a highly reflective layer and produce eyeshine as a result[14], are particularly promising targets. They are easily detectable with a light source adjacent to the detector's pupil[1] even when the source is weak (Fig. 1e).

To test this hypothesis, we visually confronted triplefins with the scorpionfish *Scorpaena porcus* (Fig. 1d), a highly cryptic, sit-and-wait predator that features eyeshine during the day to camouflage its pupil[12] (Fig 1e-f). The retroreflective component of the eyeshine was defined as narrow-sense *stratum argenteum reflected* (SAR) eyeshine[12].

We experimentally suppressed ocular spark generation in triplefins by gluing opaque mini-hats onto their heads (Fig. 1c). Two controls permitted regular ocular spark formation: a clear-hatted (Fig. 1b) and an unhatted sham control (Fig. 1a). Triplefins were tested in triplets that included one individual of each treatment. A pilot experiment confirmed that typical behaviours such as fin flicks,

push-ups, active movement across the substrate, and head and eye movements did not differ between treatments[15].

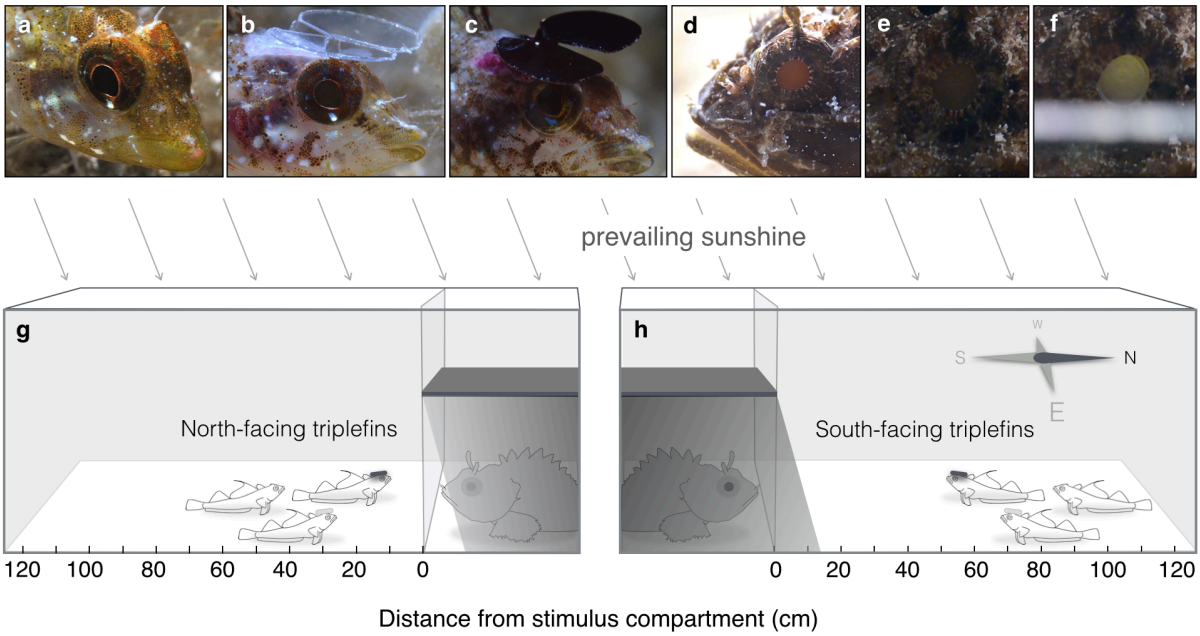

Fig. 1 | Experimental manipulation and design. Triplefins (*Tripterygion delaisi*) were subjected to one of three treatments: **a**, Unhatted sham control, **b**, Clear-hatted control, and **c**, Shading hat. Whereas **a** and **b** can re-direct light using ocular sparks, visible as bright white dots on the lower iris, **c** cannot. **d**, Their cryptobenthic predator, the scorpionfish *Scorpaena porcus*, which shows retroreflective eyeshine[12] when illuminated coaxially, here by means of a strip of paper (compare **e**-**f**). Triplets of triplefins containing one fish from each treatment were visually exposed to a predator (deterrent) or a stone (attractant, not shown) (**g**-**h**, not to scale). Distance from the stimulus was the response variable. (Pictures by M.S. and N.K.M.)

In a laboratory experiment, we visually exposed triplefins to a scorpionfish and a stone in an otherwise stone-free aquarium for two days, but only one of the two stimuli was visible on a given day. Given their preference for rocky substrates, the stone served as an attractor and positive control, whereas the scorpionfish was predicted to have a deterrent effect. We noted the distance to the visual stimulus five times per day. The results show that all individuals were positioned farther from the predator than from the stone (Fig. 2). A comparison of the two controls (unhatted and clear hatted) (Fig. 2a) showed this stimulus effect was independent of the hat treatment (Linear Mixed Effects Model LMEM: $R^2_{marg} = 0.30$, $R^2_{cond} = 0.31$, hat treatment $p = 0.66$, stimulus $p < 0.0001$, hat treatment x stimulus $p = 0.41$, stimulus order $p = 0.10$). A subsequent comparison of the pooled controls against the shading hat treatment (Fig. 2b) showed the same overall effect of the stimulus (LMEM: $R^2_{marg} = 0.28$, $R^2_{cond} = 0.28$: hat treatment $p < 0.0001$, stimulus $p < 0.0001$, stimulus order $p = 0.04$), but now the effect depended on hat treatment (hat treatment x stimulus $p = 0.016$). Relative to the controls, shaded individuals stayed significantly closer to the scorpionfish (LMEM for stimulus

scorpionfish: R^2_{marg} = 0.14, R^2_{cond} = 0.23: hat treatment $p < 0.0001$, stimulus order $p = 0.31$) but not to the stone (LMEM for stimulus stone: R^2_{marg} = 0.02, R^2_{cond} = 0.02: hat treatment $p = 0.21$, stimulus order $p = 0.16$).

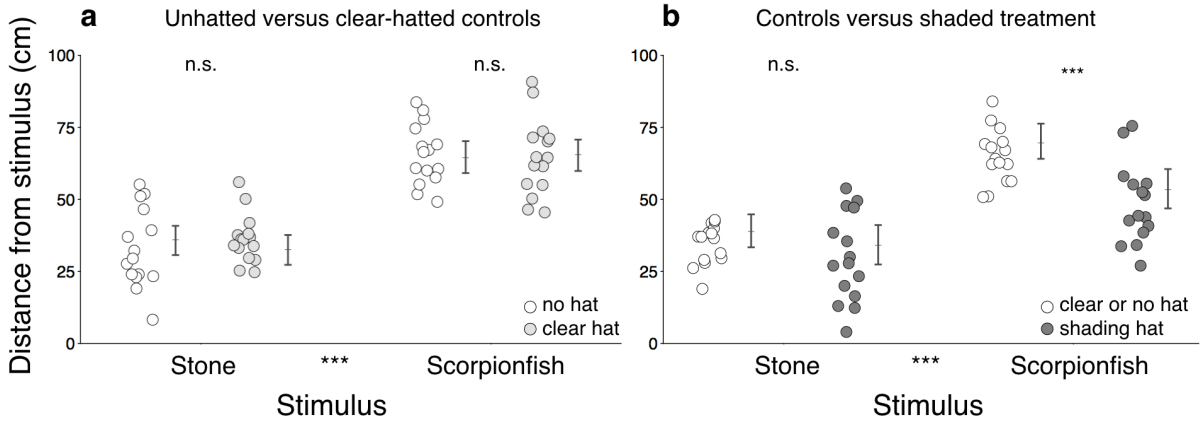

Fig. 2 | **Consequences of hatting on visual detection in the laboratory**. Distance from the stimulus as a function of stimulus type (stone or scorpionfish) and hat treatment. **a**, Controls did not differ in how much they were attracted to the stone or deterred by the scorpionfish. **b**, Relative to the pooled controls, shaded individuals stayed significantly closer to the scorpionfish. Symbols = average of 5 measurements per triplet; n = 15 triplets; error bars: model-predicted means ± 95 % credible intervals; *** = $p < 0.001$, n.s. = $p > 0.05$ (see text and methods for details).

In a field-replicate of the experiment we placed 10 translucent tanks on the sea floor at 15 m depth (Fig. 1g-h). In consideration for the possible effect of orientation in relation to the sun, five tanks were oriented north, another five south (Fig. 1h). The distance to the stimulus was determined while SCUBA diving three times per day. Once more, the response of the two controls did not differ (Fig. 3a), but the response to the predator was stronger in the tanks facing south (LMEM: R^2_{marg} = 0.31, R^2_{cond} = 0.56: hat treatment $p = 0.670$, stimulus $p < 0.0001$, hat treatment x stimulus $p = 0.48$, orientation $p = 0.37$, stimulus x orientation $p < 0.0001$, stimulus order $p = 0.004$). When comparing pooled controls against the shading treatment in the north-facing triplefins (Fig. 3b), the predator once more acted as a strong deterrent compared to the stone (LMEM: R^2_{marg} = 0.23, R^2_{cond} = 0.45: hat treatment $p = 0.75$, stimulus $p < 0.0001$, stimulus order $p < 0.0001$), but this time, the effect varied between hat treatments (hat treatment x stimulus $p = 0.037$): relative to the pooled controls, shaded individuals stayed significantly closer to the scorpionfish (LMEM for scorpionfish: R^2_{marg} = 0.03, R^2_{cond} = 0.61: hat treatment $p = 0.009$, stimulus order $p = 0.544$) but not when exposed to a stone (LMEM stone: R^2_{marg} = 0.16, R^2_{cond} =0.73: hat treatment $p = 0.094$, stimulus order $p = 0.025$). In south-facing triplefins (Fig. 3b), the same overall stimulus was present. However, shaded individuals did not differ in response when compared to the pooled controls, regardless of the stimulus (LMEM: R^2_{marg} = 0.39, R^2_{cond} =0.58, hat treatment $p = 0.119$, stimulus $p < 0.0001$, hat treatment x stimulus $p = 0.247$). In

112 south-facing triplefins, light conditions may have been optimal for the detection of the camouflaged
113 scorpionfish through regular vision, precluding the benefits of active photolocation.
114

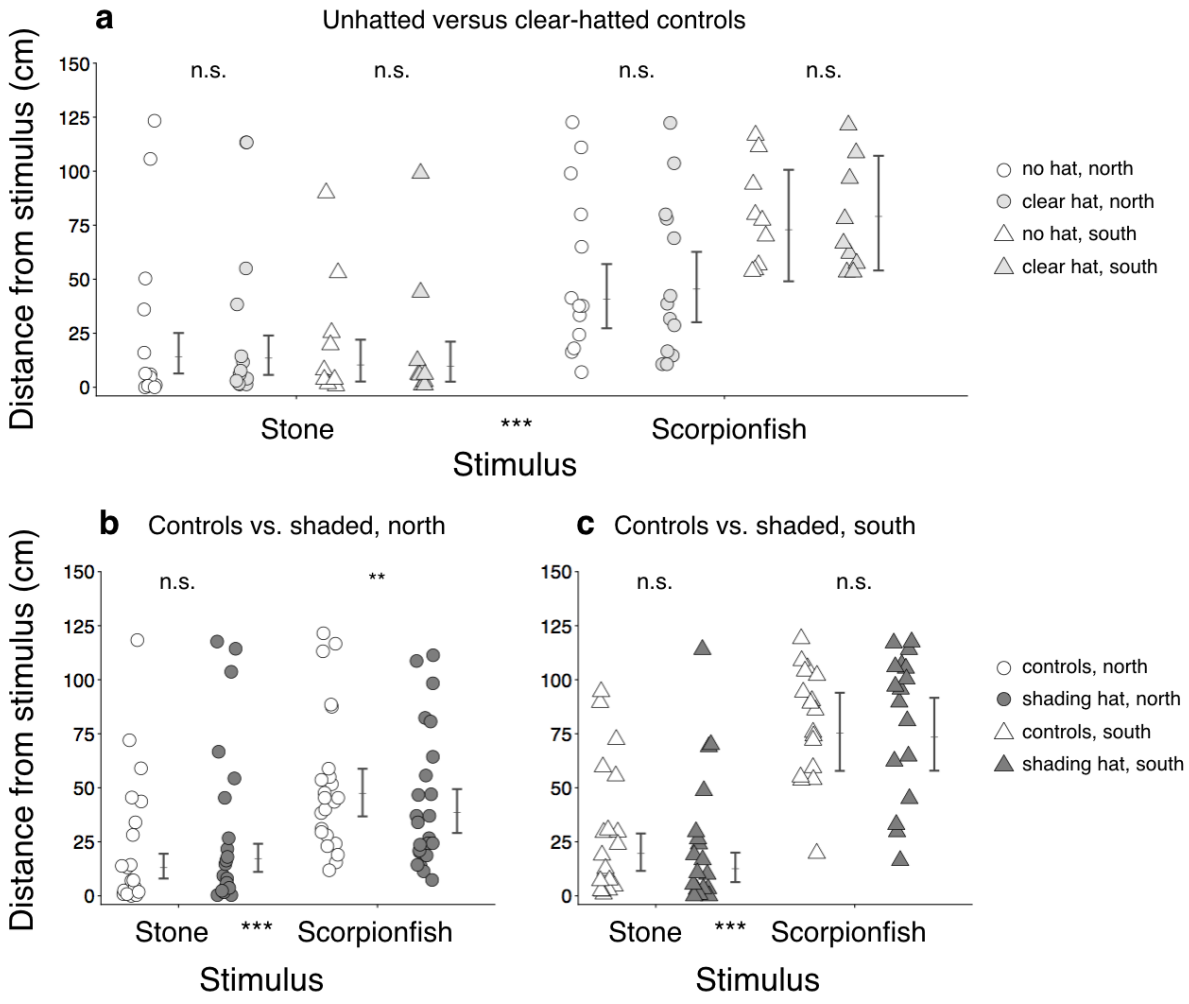

115

116 **Fig. 3** | **Consequences of hatting on visual detection in the field.** Distance from stimulus as a function of
117 stimulus type (stone of scorpionfish) and hat treatment. **a**, Controls did not differ in their response, but south-
118 facing controls responded stronger (n = 22 triplets). **b**, In north-facing triplefins, shaded fish stayed closer to a
119 scorpionfish than the controls (n = 21 triplets). **c**, In south-facing triplefins, such effect was absent (n = 19
120 triplets). Symbols: average of 3 measurements per individual; error bars: model-predicted means ± 95 %
121 credible intervals. *** = $p < 0.001$, n.s. = $p > 0.05$ (see text and methods for details).

122

123 To validate our experimental results, we implemented visual models to compare the
124 radiance of the pupil of a scorpionfish as perceived by a triplefin with and without an ocular spark.
125 Such change in radiance can be caused either by the triplefin switching its ocular spark on or off, or
126 by the scorpionfish changing its gaze. We limited ourselves to modelling blue ocular sparks (Fig. 1a,
127 b), which have an average reflectance (expressed as proportion) of 0.99 over the 400-700 nm range,
128 with a maximum of 1.55 at 472 nm, illustrating the effect of light focussing[3] by the lens. Further
129 parameters included ambient light estimates in the field tanks, scorpionfish pupil size, baseline

radiance (Fig. 1d) and reflective properties[12], and the triplefin visual system[4]. We used the receptor-noise model[16] for estimating chromatic contrasts and computed Michelson contrasts using cone-catch values for achromatic contrasts.

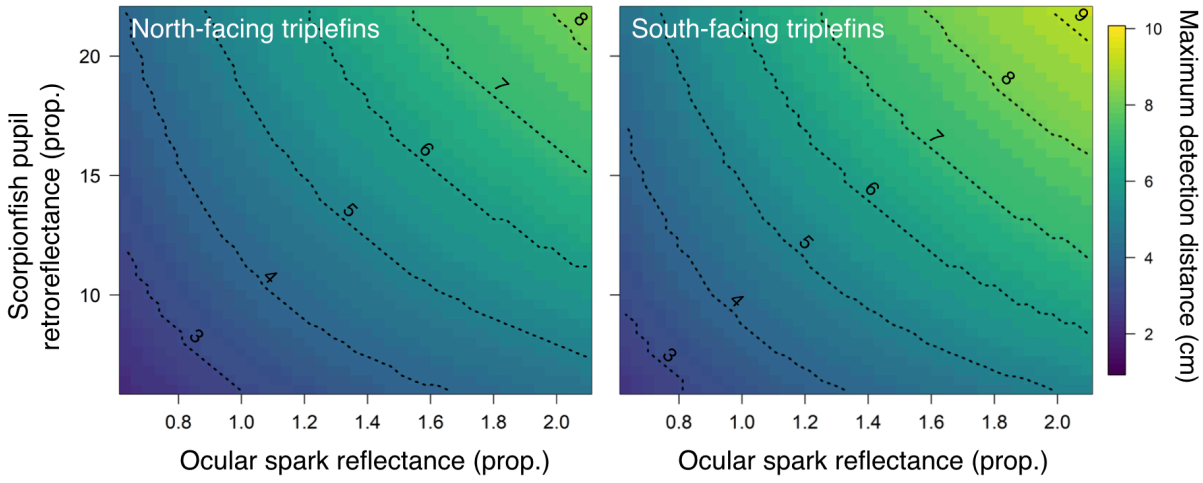

Fig. 4 | Theoretical active photolocation detection distance of a scorpionfish's eye by a triplefin. Visual modelling output showing maximum detection distance (colour) of achromatic contrast differences in a scorpionfish's pupil as triggered by a triplefin's blue ocular spark. The outcome is shown as a function of ocular spark reflectance and scorpionfish pupil retroreflectance, separated by triplefin orientation (Fig. 1g-h). Values were obtained from calculating the Michelson contrast based on triplefins' cone-catches for each millimetre between 1 and 15 cm, and identifying the maximum distance at which the contrast was equal to or exceeded the achromatic contrast threshold of *T. delaisi* (0.8 %). Both axes cover the range of measured values.

Ocular sparks did not generate a chromatic contrast above discriminability threshold at any distance between the triplefin and scorpionfish but produced detectable achromatic contrasts across a broad range of conditions (Fig. 4). For north-facing triplefins, the reflection of the ocular spark from a scorpionfish's pupil would be detectable from ~5 cm under average conditions. In situations when ocular spark radiance and scorpionfish eye retroreflectance have greater value, the reflection of the ocular spark would be detectable from over 8 cm. The calculated detection distances increase slightly for triplefins facing south. Recognising a predator at these distances is likely to reduce the probability of capture by scorpionfish since they strike over short distances only[17-19]. For comparison, identical calculations for spark-generated contrast changes in a scorpionfish's iris rather than pupil showed no perceptible effect under any of the tested conditions.

Our results provide convincing evidence for the diurnal active photolocation hypothesis by showing that small benthic fish can significantly increase the distance at which they detect life-threatening predators by redirecting downwelling light. The properties described here for the triplefin and the scorpionfish are not unique: mechanisms for light redirection are widespread and diverse across diurnal fish families[3,13], as are retroreflective eyes featured by cryptic predators[12].

Diurnal active photolocation could be an important, yet previously neglected, vision enhancement mechanism, and thereby represent a significant force in the evolution of fish eyes.

Methods

Model species

Tripterygion delaisi is a small (4–5 cm) NE-Atlantic and Mediterranean micro-predatory fish species found in rocky substrates at 5 to 20 m depth (max 1 to 50 m). Aside from breeding males, it is highly cryptic and regularly produces blue and red ocular sparks[3]. *Scorpaena porcus* is a cryptobenthic sit-and-wait predator (12–20 cm) from coastal marine hard substrates and seagrass habitats within the NE-Atlantic and Mediterranean Sea[20]. Small benthic fish, like triplefins, are often a component of its diet[21]. It possesses a reflective stratum argenteum and partially translucent retinal pigment epithelium that allows for the generation of daytime eyeshine, which is considered to be a form of pupil camouflage[12]. All experiments were conducted in Calvi (Corsica, France) under the general permit of STARESO (Station de Recherches Sous Marines et Océanographiques).

Hatting technique to block ocular sparks

We prevented downwelling light from reaching the iris to inhibit ocular sparks by fitting triplefins with plastic micro-hats from polyester filters excised using a laser cutter (RLS 100, AM Laserpoint Deutschland GmbH, Hamburg, Germany). A dark red filter with average transmission 1 % was used for the shading treatment (LEE Filters #787 “Marius Red”, LEE Filters, UK). Clear filter hats (LEE Filters #130, “Clear”) were used in the first control group, and no hat, but the same handling procedure, in the second control group. Hats were individually adjusted with clippers and folded into their final configuration with a triangular base for attachment and forward-projecting, raised wings to shade the eyes from downwelling light only. Hats allowed full eye movement in all directions (Fig. 1b-c) and varied from 6 to 9 mm in diameter, matching individual head size. Animals in both control groups regularly generated ocular sparks both in the laboratory and in the field.

T. delaisi were collected using hand nets while SCUBA diving and brought to a stock aquarium in the laboratory. Individuals were anaesthetised (100 mg L^{-1} MS-222 in seawater, pH = 8.2) until all movements ceased except for breathing (3–4.5 min). Subsequently, the dorsal head surface was gently dried with paper tissue. Hats were glued to the triangular dorso-posterior head area just behind the eyes using surgical glue (Surgibond, Sutures Limited, UK). After allowing the glue to polymerise for 45 s, fish were moved into recovery containers with aerated seawater. Individuals

regained consciousness and mobility within 5–10 min. This non-invasive hat fixation protocol minimised impacts on the fish's natural behaviour and health, as indicated by a 97.4 % survival rate. As a trade-off, however, hats detached within 0–4 days, which reduced the number of triplets that could be used for analysis (see Statistical analysis). All fish were treated and included in trials once and only returned to the field after completion of the experiment.

Laboratory experiment

Four tanks (L × W × D: 130 × 50 × 50 cm^3) were used for 20 experimental runs, each employing a new triplet of size-matched *T. delaisi*. In each tank, we placed a rock and a scorpionfish in two separate perforated containers (L × W × H: 24 × 14 × 16 cm^3) with a glass front. Both stimuli were simultaneously present in the tank, but only one was visible to the triplefins. The bottom of the aquarium was barren (avoided by the fish), except for a 10 cm strip of gravel placed along the long side of the tank, providing a sub-optimal substrate. Each tank was illuminated with a 150 W cold white LED floodlight (TIROLED Hallenleuchte, 150 W, 16000 Lumen) shielded with a LEE Filters #172 Lagoon Blue filter to simulate light at depth. The area of the tank where stimuli were displayed was shaded. All triplets were exposed to each stimulus for one full day. Since fish are moving regularly, we assessed the distance to the stimulus five times per day, at 0800, 1100, 1300, 1500 and 1800. Stimuli were presented in random order.

Field experiment

We replicated the experiment in the field using ten tanks of spectrally neutral Evotron Plexiglas (L × W × D: 150 × 25 × 50 cm^3) placed at 15 m depth on sandy patch in the seagrass meadow in front of STARESO. We used local silica sand mixed with gravel as substrate. Visual contact between tanks was excluded by surrounding each enclosure with 10 cm white side covers. As a response variable, we noted the distance of each individual from the stimulus compartment three times a day at 0900, 1200 and 1500 for two days following deployment in the early evening of the first day. Stimuli were always changed after the first observation day. Triplets were replaced every three days. In total, 75 triplets were tested.

Statistical analysis

Behavioural data were analysed using Linear Mixed Effects Models (LMEM) with the lme4 package[22] for R v3.3.2.[23]. For both experiments, we first compared the two control treatments (sham and clear hat) to verify that hatting a fish did not affect behaviour, and to confirm their ability to distinguish a

cryptic predator from a stone. Because controls did not differ, we pooled their data for the final models and compared them to the shaded treatment. This allowed us to include triplets in which only the clear-hatted fish had lost its hat for the comparison with the shaded fish (such triplets were excluded from the comparison of the controls). This accounts for the variation in triplet numbers in the final analyses. Distance from the display compartment was used as the response variable in both models.

For the laboratory experiment, the initial fixed model components included the main predictors *stimulus* (stone *vs* scorpionfish), *hat treatment* (no hat *vs* clear hat, or pooled controls *vs* shaded) and their interaction. We further included the fixed covariates *daytime*, *stimulus order, cohort and tank ID.* The models for the replicated field experiment were identical, but also included the fixed factor *orientation* (north or south) and its interactions with the main factors. We also square-root-transformed the response variable *distance* to improve residual homogeneity. The transformation of the response variable did not cause any change in the effects of the interactions between covariates. Models to compare the response of controls *vs* shaded fish were calculated separately for north *vs* south orientation because fish responded differently to the scorpionfish depending on orientation (Fig. 3).

In all models, the initial random component contained triplet ID with random slopes over the hat treatment. This accounts for the repeated measurements of each triplet and captures variation arising from different hat-treatment responses among triplets[24]. Random slopes were not informative and subsequently removed. We then performed backward model selection using the Akaike's Information Criterion (AIC) to identify the best-fitting model with the smallest number of covariates[25]. We only report the reduced final models and provide proxies for their overall goodness-of-fit (marginal and conditional R^2) using pairwiseSEM[26]. The marginal R^2 expresses the proportion of variation explained by the model considering fixed factors only, whereas the conditional R^2 expresses the same including the random factors[27]. We used Wald *z*-tests to assess the significance of fixed effects. To explore significant interactions between stimulus and hat treatment, we implemented new models within the two levels of the stimulus treatment. Model assumptions were validated by plotting residuals versus fitted values and each covariate present in the full, non-reduced model[28].

Estimating scorpionfish pupil radiance with and without ocular spark

We assumed both triplefins and scorpionfish were looking orthogonally at one another to calculate the photon flux of the scorpionfish pupil reaching the triplefin, with and without the contribution of a blue ocular spark (**SI 1**). Using retinal quantum catch estimates, we calculated the chromatic contrast[16] between the scorpionfish pupil with and without ocular sparks. The achromatic contrast between the same two conditions was estimated by calculating the Michelson contrast for the

quantum catches of the two-long-wavelength photoreceptors. For comparison, we also performed the same calculations using photon flux of the scorpionfish iris with and without the contribution of an ocular spark. We parameterized the equations using measurements of: (1) ambient light in the tanks at 15 m depth, (2) the range of ocular spark radiance under downwelling light conditions, (3) baseline scorpionfish pupil radiance in the experimental tanks, (4) sizes of triplefin pupil, ocular spark and scorpionfish pupil, and (5) scorpionfish pupil and iris reflectance[12].

Spectroradiometric measurements were obtained with a calibrated SpectraScan PR-740 (Photo Research, New York USA) encased in an underwater housing (BS Kinetics, Germany). This device measures spectral radiance (watts sr^{-1} m^{-2} nm^{-1}) of an area with defined solid angle. The downwelling light was estimated by measuring the radiance of a polytetrafluoroethylene (PTFE) diffuse white reflectance standard (Berghof Fluoroplastic Technology GmbH, Germany) positioned parallel to the water surface from a 45° angle. Radiance values were transformed into photon radiance (photons s^{-1} sr^{-1} m^{-2} nm^{-1}).

We determined the relationship between the radiance of the ocular spark and that of a white PTFE standard exposed to downwelling light in live triplefins. Fish mildly sedated with (n = 10) were placed in an aquarium illuminated with a Leica EL 6000 source and a liquid light guide suspended ~20 cm above the tank. Spark radiance was normalised by comparing it to a white standard at 45° from normal positioned at the same location as the fish. For each fish, three measurements were obtained from each eye. The highest within-fish value relative to the standard was used for the model. The sizes of the triplefin pupil (n = 35), the ocular spark (n = 10), and the scorpionfish pupil (n = 20) were measured in ImageJ[29] using scaled images. Natural baseline pupil radiance of three different scorpionfish was measured orthogonally to the pupil from the perspective of the triplefins during the experimental trials using a Photo Research PR-740 spectroradiometer.

Solid angles of the ocular spark as perceived from the perspective of the scorpionfish, and the pupil of the scorpionfish as perceived by the triplefin, were estimated through Monte Carlo simulations using SACALC3 v1.4[30]. Source and detector were both approximated as circular disks with the source radiating equally in all directions of a hemisphere (i.e. 2π steradians).

Visual models and maximum detection distance

The receptor-noise limited model for calculation of chromatic contrast was informed using triplefin ocular media transmission values, photoreceptor sensitivity curves[4,31], and the relative photoreceptor density of single to double cone of 1:4:4 as found in the triplefin fovea[5]. We used a Weber fraction (ω) value of 0.05 as in previous studies[32,33]. Chromatic contrasts are measured as just-noticeable differences (JNDs), where values above one are considered to be larger than the minimum

discernable difference between two objects. We calculated the Michelson achromatic contrast as $(Q_1-Q_2)/(Q_1+Q_2)$ where Q_1 and Q_2 are the quantum catches of the two members of the double cones which are associated with the achromatic channel, under photon $flux_1$ and photon $flux_2$. We determined the maximum discernable distance of the ocular spark radiance returned by the scorpionfish pupil by calculating the chromatic and achromatic contrast at each millimeter, between 1 and 15 cm, and extracting the first value at which the contrast was equal to or exceeded 1.0 JND for chromatic contrasts and 0.008 for Michelson contrasts as measured in *T. delaisi* (Matteo Santon, unpublished data) and other fish species[34]. All visual models were performed using the R package pavo[35].

End notes

Supplementary Information (list)

Supplementary Information 1: Visual model details

Acknowledgements We are indebted to the attendants of a workshop in November 2014 in Tübingen: Connor M. Champ, João Coimbra, Colin B. Jack, Sönke Johnsen, Almut Kelber, Melissa G. Meadows, Daniel Osorio, Shelby Temple and Annette Werner. Thanks to Martin J. How for useful suggestions on an earlier draft. Jonas Dornbach, Thomas Griessler, Katharina Hiemer, Michael Karcz, Valentina Richter, Peter Tung, Sabine Urban, Laura Warmuth and Florian Wehrberger supported data collection in the field. Gregor Schulte provided creative and technical support. Thanks to Pierre Lejeune, director of STARESO and his staff for providing excellent working conditions. N.K.M. was supported by Koselleck Grant Mi 482/13-1 from the Deutsche Forschungsgemeinschaft and Experiment! grant Az. 89148 and Az. 91816 from the Volkswagen Foundation. P-P.B. was funded by a Postdoctoral Fellowship from the Natural Sciences and Engineering Research Council of Canada.

Author contributions N.K.M., R.F., M.S., P-P.B. and U.K.H. conceived the study. R.F. developed the hatting technique. N.K.M., J.D., M.S., U.K.H., R.F. and P-P.B. conceptualised the experiments. J.D. collected the laboratory data. M.S. and U.K.H. collected the field data, with assistance from the whole crew. M.S. and N.A. analysed the experimental data. P-P.B. developed and ran the visual model with support from M.S. using spectroradiometric data collected by M.S. and U.K.H. The manuscript was written by N.K.M., M.S., P.-P.B., R.F. and J.D. All authors edited and approved the manuscript.

Competing interests All authors declare that they have no competing interests.

Additional information

Supplementary information is available for this paper at *<< attached to end of this file >>*

Correspondence and requests for materials should be addressed to N.K.M.

1. Howland, H. C., Murphy, C. J. & McCosker, J. E. Detection of eyeshine by flashlight fishes of the family Anomalopidae. *Vision Res.* **32**, 765-769, doi:10.1016/0042-6989(92)90191-k (1992).
2. Hellinger, J. *et al.* The Flashlight Fish *Anomalops katoptron* Uses Bioluminescent Light to Detect Prey in the Dark. *PLoS ONE* **12**, e0170489, doi:10.1371/journal.pone.0170489 (2017).
3. Michiels, N. K. *et al.* Controlled iris radiance in a diurnal fish looking at prey. *R. Soc. open sci.* **5**, 170838, doi:10.1098/rsos.170838 (2018).
4. Bitton, P.-P. *et al.* Red fluorescence of the triplefin *Tripterygion delaisi* is increasingly visible against background light with increasing depth. *R. Soc. open sci.* **4**, 161009, doi:10.1098/rsos.161009 (2017).
5. Fritsch, R., Collin, S. P. & Michiels, N. K. Anatomical analysis of the retinal specializations to a crypto-benthic, micro-predatory lifestyle in the mediterranean triplefin blenny *Tripterygion delaisi*. *Front. Neuroanat.* **11**, 122, doi:10.3389/fnana.2017.00122 (2017).
6. Sutton, T. T. Trophic ecology of the deep-sea fish *Malacosteus niger* (Pisces: Stomiidae): An enigmatic feeding ecology to facilitate a unique visual system? *Deep-Sea Res. Part I Oceanogr. Res. Pap.* **52**, 2065-2076, doi:10.1016/j.dsr.2005.06.011 (2005).
7. Douglas, R. H., Mullineaux, C. W. & Partridge, J. C. Long-wave sensitivity in deep-sea stomiid dragonfish with far-red bioluminescence: evidence for a dietary origin of the chlorophyll-derived retinal photosensitizer of *Malacosteus niger*. *Philos. Trans. R. Soc. Lond. B Biol. Sci* **355**, 1269-1272, doi:10.1098/rstb.2000.0681 (2000).
8. Douglas, R. H. *et al.* Enhanced retinal longwave sensitivity using a chlorophyll-derived photosensitiser in *Malacosteus niger*, a deep-sea dragon fish with far red bioluminescence. *Vision Res.* **39**, 2817-2832, doi:10.1016/S0042-6989(98)00332-0 (1999).
9. Kenaley, C. P., Devaney, S. C. & Fjeran, T. T. The complex evolutionary history of seeing red: molecular phylogeny and the evolution of an adaptive visual system in deep-sea dragonfishes (Stomiiformes: Stomiidae). *Evolution* **68**, 996-1013, doi:10.1111/evo.12322 (2014).
10. Sutton, T. T. & Hopkins, T. L. Trophic ecology of the stomiid (Pisces: Stomiidae) fish assemblage of the eastern Gulf of Mexico: Strategies, selectivity and impact of a top mesopelagic predator group. *Mar. Biol.* **127**, 179-192, doi:10.1007/bf00942102 (1996).
11. Jack, C. B. *Detecting the Detector: A Widespread Animal Sense?*, <http://vixra.org/abs/1411.0226> (2014).
12. Santon, M., Bitton, P. P., Harant, U. K. & Michiels, N. K. Daytime eyeshine contributes to pupil camouflage in a cryptobenthic marine fish. *Sci. Rep.* **8**, 7368, doi:10.1038/s41598-018-25599-y (2018).
13. Anthes, N., Theobald, J., Gerlach, T., Meadows, M. G. & Michiels, N. K. Diversity and ecological correlates of red fluorescence in marine fishes. *Front. Ecol. Evol.* **4**, doi:10.3389/fevo.2016.00126 (2016).

14. Fritsch, R., Ullmann, J. F. P., Bitton, P. P., Collin, S. P. & Michiels, N. K. Optic-nerve-transmitted eyeshine, a new type of light emission from fish eyes. *Front. Zool.* **14**, 14, doi:10.1186/s12983-017-0198-9 (2017).
15. Dehm, J. *Does wearing a hat change the demeanour of a fish? A behavioural study of the manipulation of active photolocation in the benthic fish Tripterygion delaisi* MSc thesis, University of Kiel, (2015).
16. Vorobyev, M. & Osorio, D. Receptor noise as a determinant of colour thresholds. *Proc. R. Soc. B Biol. Sci.* **265**, 351-358, doi:DOI 10.1098/rspb.1998.0302 (1998).
17. Montgomery, J. C. & Hamilton, A. R. Sensory contributions to nocturnal prey capture in the dwarf scorpion fish (*Scorpaena papillosus*). *Mar. Fresh. Behav. Physiol.* **30**, 209-223, doi:Doi 10.1080/10236249709379026 (1997).
18. La Mesa, M., Scarcella, G., Grati, F. & Fabi, G. Age and growth of the black scorpionfish, *Scorpaena porcus* (Pisces: Scorpaenidae) from artificial structures and natural reefs in the Adriatic Sea. *Sci. Mar.* **74**, 677-685 (2010).
19. Harmelin-Vivien, M., Kaim-Malka, R., Ledoyer, M. & Jacob-Abraham, S. Food partitioning among scorpaenid fishes in Mediterranean seagrass beds. *J. Fish Biol.* **34**, 715-734 (1989).
20. Louisy, P. *Europe and Mediterranean marine fish identification guide*. (Ulmer, 2015).
21. Compaire, J. C., Casademont, P., Cabrera, R., Gómez-Cama, C. & Soriguer, M. C. Feeding of *Scorpaena porcus* (Scorpaenidae) in intertidal rock pools in the Gulf of Cadiz (NE Atlantic). *J. Mar. Biol. Assoc. U. K.*, 1-9 (2017).
22. Bates, D., Mächler, M., Bolker, B. M. & Walker, S. Fitting linear mixed-effects models using lme4. *J. Stat. Softw.* **67**, 1-51 (2014).
23. R-Core-Team. *R: A language and environment for statistical computing*. (R Foundation for Statistical Computing, vienna, Austria, 2013).
24. Schielzeth, H. & Forstmeier, W. Conclusions beyond support: overconfident estimates in mixed models. *Behav. Ecol.* **20**, 416-420, doi:10.1093/beheco/arn145 (2009).
25. Zuur, A. F., Ieno, E. N., Walker, N. J., Saveliev, A. A. & Smith, G. M. *Mixed Effects Models and Extensions in Ecology with R*. (Springer, New York, 2009).
26. Lefcheck, J. S. & Freckleton, R. piecewiseSEM: Piecewise structural equation modelling inr for ecology, evolution, and systematics. *Methods Ecol. Evol.* **7**, 573-579, doi:10.1111/2041-210x.12512 (2016).
27. Nakagawa, S. & Schielzeth, H. Repeatability for Gaussian and non-Gaussian data: a practical guide for biologists. *Biol. Rev.* **85**, 935-956, doi:10.1111/j.1469-185X.2010.00141.x (2010).
28. Zuur, A. F., Ieno, E. N. & Freckleton, R. A protocol for conducting and presenting results of regression-type analyses. *Methods Ecol. Evol.* **7**, 636-645, doi:10.1111/2041-210x.12577 (2016).
29. Abràmoff, M. D., Magalhães, P. J. & Ram, S. J. Image processing with ImageJ. *Biophotonics Int.* **11**, 36-42 (2004).
30. Whitcher, R. A Monte Carlo method to calculate the average solid angle subtended by a right cylinder to a source that is circular or rectangular, plane or thick, at any position and orientation. *Radiat. Prot. Dosim.* **118**, 459-474, doi:10.1093/rpd/nci381 (2006).
31. Govardovskii, V. I., Fyhrquist, N., Reuter, T., Kuzmin, D. G. & Donner, K. In search of the visual pigment template. *Visual Neurosci.* **17**, 509-528, doi:10.1017/s0952523800174036 (2000).
32. Wilkins, L., Marshall, N. J., Johnsen, S. & Osorio, D. Modelling colour constancy in fish: implications for vision and signalling in water. *J. Exp. Biol.* **219**, 1884-1892, doi:10.1242/jeb.139147 (2016).
33. Matz, M. V., Marshall, N. J. & Vorobyev, M. Are corals colorful? *Photochem. Photobiol* **82**, 345-350, doi:10.1562/2005-08-18-RA-653 (2006).
34. Douglas, R. & Djamgoz, M. *The visual system of fish*. (Springer Science & Business Media, 2012).
35. Maia, R., Eliason, C. M., Bitton, P. P., Doucet, S. M. & Shawkey, M. D. pavo: an R package for the analysis, visualization and organization of spectral data. *Methods Ecol. Evol.* **4**, 906-913, doi:10.1111/2041-210x.12069 (2013).

Supplemental Information 1

Visual model details

Table S1 | Symbols and abbreviations used in the equations to calculate the photon flux of the scorpionfish pupil reaching the triplefin, with and without the contribution of an ocular spark

Symbol	***Definitions and units***
L	Photon radiance (photons s^{-1} sr^{-1} m^{-2})
S	Blue ocular spark reflectance (proportion in relation to PTFE white standard)
d	Distance between triplefin and scorpionfish (m)
r_t	Radius of triplefin pupil (m)
R	Reflectance of coaxially illuminated scorpionfish pupil (prop. in relation to PTFE white standard)
κ	Diffuse attenuation coefficient (m^{-1})
Φ	Photon flux (photons s^{-1})
Ω	Solid angle (sr)

Triplefin – scorpionfish interaction

The starting condition assume that both fish look at each other at normal incidence, i.e. the full area of the pupil of the triplefin is visible to the scorpionfish and vice versa. Solid angles are computed assuming the ocular spark is positioned at the edge of the iris (displacement = 1.09 mm) in the plane of the triplefin pupil.

Photon flux without ocular spark

The photon radiance of the scorpionfish pupil reaching the triplefin (L_d) is a function of the measured scorpionfish pupil photon radiance (L_0) attenuated by the aquatic medium over distance *d* such that

$$L_d = L_0 \times e^{-\kappa d} \quad (1)$$

The photon flux reaching the retina of the triplefin without the ocular spark (Φ_{ns}) is the proportion of attenuated photon radiance reaching the triplefin's pupil (L_d) multiplied by the solid angle of the scorpionfish pupil (Ω_{sp}) and the area of the triplefin pupil (πr_t^2):

$$\Phi_{ns} = L_d \times \Omega_{sp} \times \pi r_t^2 \quad (2)$$

448 *Photon flux with ocular spark*

449 The photon radiance of the ocular spark reaching the scorpionfish (L_{os}) is a function of the radiance
450 of a PTFE white standard parallel to the water surface (L_w), the focussing power of the lens, and the
451 reflective properties of the iridal chromatophores on which the light is focused. For now, the
452 focussing power and reflective properties have only been measured together as blue ocular spark
453 reflectance (S):

454 $$L_{os} = L_w \times S \times e^{-\kappa d} \quad (3)$$

455

456 The radiance of the scorpionfish pupil (L_{sp}) defined as the proportion of the attenuated ocular spark
457 photon radiance that reaches the scorpionfish pupil and is re-emitted towards the triplefin is
458 estimated by multiplying the photon radiance of the ocular spark reaching the scorpionfish (L_{os}) with
459 the solid angle of the ocular spark as seen by the scorpionfish (Ω_{os}) and the retroreflectance of the
460 scorpionfish pupil with illumination co-axial to the receiver (R). Because the properties of the
461 retroreflective eye are measured in relation to a diffuse white standard, the photon exitance from
462 the scorpionfish pupil is converted to photon radiance by dividing by π steradians:

463 $$L_{sp} = L_{os} \times \Omega_{os} \times R \times \pi^{-1} \quad (3)$$

464

465 The scorpionfish pupil radiance (L_{sp}) travelling towards the triplefin pupil is further attenuated, and
466 the photon flux reaching the triplefin's retina (Φ_{os}) is obtained by multiplying the attenuated
467 radiance by the solid angle of the scorpionfish pupil, and the area of the triplefin pupil:

468 $$\Phi_{os} = L_{sp} \times e^{-\kappa d} \times \Omega_{sp} \times \pi r_t^2 \quad (4)$$

469

470 The photon flux generated by the ocular spark, which reaches the triplefin retina after being
471 reflected by the scorpionfish pupil is therefore approximated by:

472 $$\Phi_{os} = L_w \times S \times e^{-\kappa d} \times \Omega_{os} \times R \times \pi^{-1} \times e^{-\kappa d} \times \Omega_{sp} \times \pi r_t^2 \quad (5)$$

473

474 The total photon flux reaching the retina of the triplefin with the ocular spark is then the sum of
475 equations (2) and (5).

476

477 The solid angle of the scorpionfish pupil from the perspective of the triplefin eye (Ω_{sp}), and the solid
478 angle of the ocular spark from the perspective of the scorpionfish eye (Ω_{os}) at distance *d* was
479 estimated by Monte Carlo simulations[30].

480

481